The EMBO Journal Vol.18 No.10 pp.2886–2896, 1999

Mutations which alter the elbow region of $tRNA_2^{Gly}$ reduce T4 gene *60* translational bypassing efficiency

Alan J.Herr, John F.Atkins and Raymond F.Gesteland[1]

Department of Human Genetics, 15N 2030 E RM 6160, University of Utah, Salt Lake City, UT 84112-5330, USA

[1]Corresponding author
e-mail: rayg@howard.genetics.utah.edu

Translating ribosomes bypass a 50 nucleotide coding gap in bacteriophage T4 gene *60* mRNA between codons 46 and 47 in order to synthesize the full-length protein. Bypassing of the coding gap requires peptidyl-$tRNA_2^{Gly}$ detachment from a GGA codon (codon 46) followed by re-pairing at a matching GGA codon just before codon 47. Using negative selection, based on the *sacB* gene from *Bacillus subtilis*, *Escherichia coli* mutants were isolated which reduce bypassing efficiency. All of the mutations are in the gene for $tRNA_2^{Gly}$. Most of the mutations disrupt the hydrogen bonding interactions between the D- and T-loops (G18•ψ55 and G19•C56) which stabilize the elbow region in nearly all tRNAs. The lone mutation not in the elbow region destabilizes the anticodon stem at position 40. Previously described *Salmonella typhimurium* mutants of $tRNA_2^{Gly}$, which reduce the stability of the T-loop, were also tested and found to decrease bypassing efficiency. Each $tRNA_2^{Gly}$ mutant is functional in translation ($tRNA_2^{Gly}$ is essential), but has a decoding efficiency 10- to 20-fold lower than wild-type. This suggests that rigidity of the elbow region and the anticodon stem is critical for both codon–anticodon stability and bypassing.

Keywords: codon–anticodon stability/sacB/translational bypassing/tRNA structure

Introduction

Unerring protein synthesis depends on correct tRNA–mRNA pairing. Cognate codon–anticodon interactions are stabilized by the ribosome in both the A-site and the P-site in order to minimize translation errors. While stabilization in the A-site ensures incorporation of correct amino acids in the polypeptide chain, stabilization in the P-site helps the ribosome maintain the correct reading frame between translocation and the next decoding step. Yet some genes require a temporary destabilization of peptidyl-tRNA–mRNA pairing in the ribosome for proper expression. These genes carry cryptic signals in their mRNAs which facilitate peptidyl-tRNA detachment from a specific codon and re-pairing at an alternate identical or synonymous codon (Atkins and Gesteland, 1995; Farabaugh, 1996). Since in most cases the alternate codon overlaps the first codon, the result is a programmed change in reading frame [examples include the +1 frameshift found in RF2 (Craigen and Caskey, 1986; Weiss *et al*., 1988) or –1 frameshifts found in many retroviruses (Brierley, 1995; Gesteland and Atkins, 1996)]. But in some cases, called translational bypassing, the peptidyl-tRNA re-pairs at a non-overlapping codon. The existence of prokaryote examples (Weiss *et al*., 1987; Huang *et al*., 1988; O'Connor *et al*., 1989; Kane *et al*., 1992; Manch-Citron and London, 1994; Gallant and Lindsley, 1998), along with a recent report showing bypassing in the expression of rabbit β-globin (Chittum *et al*., 1998), indicates that this phenomenon may be common to most organisms.

The best characterized example of translational bypassing is in gene *60* of bacteriophage T4 (Weiss *et al*., 1990), encoding a topoisomerase subunit. In this case, the peptidyl-tRNA ($tRNA_2^{Gly}$) detaches from a GGA codon (codon 46) and re-pairs at a second GGA codon 47 nucleotides downstream. To stimulate bypassing of this non-coding information (or coding gap), gene *60* mRNA relies on several *cis*-acting signals (Figure 1). These signals include matching GGA codons (referred to as take-off and landing sites) flanking an optimally sized coding gap, a stop codon immediately downstream of the take-off site, a stem–loop structure in the 5′ end of the coding gap, and a stretch of basic and hydrophobic amino acids translated from codons preceding the coding gap.

Modulation of peptidyl-$tRNA_2^{Gly}$ pairing with the crucial GGA codon is at the center of the proposed model for bypassing: peptidyl-$tRNA_2^{Gly}$ releases from the take-off site GGA, the mRNA moves through the ribosome, and peptidyl-$tRNA_2^{Gly}$ re-pairs at the landing site GGA. Peptidyl-$tRNA_2^{Gly}$ appears to locate the landing site by scanning the coding gap for a cognate codon as the mRNA moves through the ribosome (F.M.Adamski, M.B.Moore, R.F.Gesteland and J.F.Atkins, in preparation). Recent estimates show that 50% of ribosomes bypass the coding gap (productive bypassing) (Maldonado and Herr, 1998). The other 50% either terminate at the UAG codon just after the take-off site, resume translation in an unproductive reading frame, or abort landing by releasing the mRNA or the peptidyl-tRNA (unproductive bypassing).

How the combination of signals stimulates bypassing remains a mystery. One possible function for the signals is to switch the ribosome into a scanning mode which allows the mRNA to move through the decoding center. Another possibility is that the signals target components of the translational apparatus which stabilize peptidyl-tRNA pairing. Previous genetic studies identified mutations in the C-terminal domain of ribosomal protein L9 which suppress mutations in the stem–loop and nascent peptide, suggesting that perhaps L9 is the target of these signals (Herbst *et al*., 1994; Adamski *et al*., 1996). Here, we report a novel set of mutations in $tRNA_2^{Gly}$ which reduce the bypassing efficiency of wild-type gene *60*.

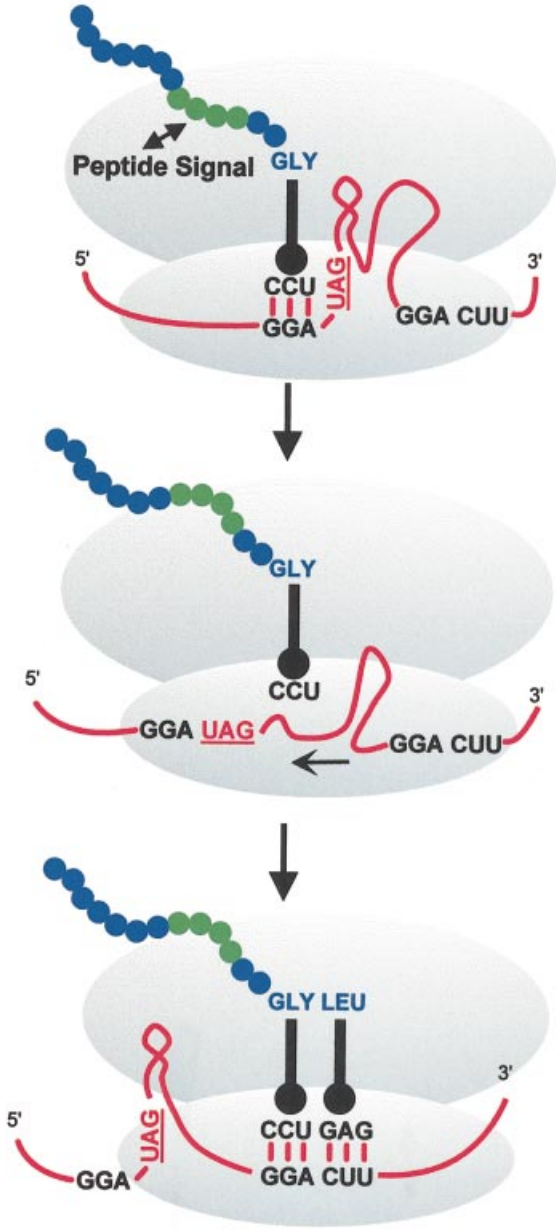

Fig. 1. Efficient translational bypassing of the gene *60* coding gap requires matching take-off and landing site GGA codons, a stop codon, a stem–loop structure, and a nascent peptide signal. In the current model, peptidyl-tRNA$_2^{Gly}$ dissociates from the take-off site GGA, scans the mRNA as it moves through the decoding center, and re-pairs with the landing site GGA.

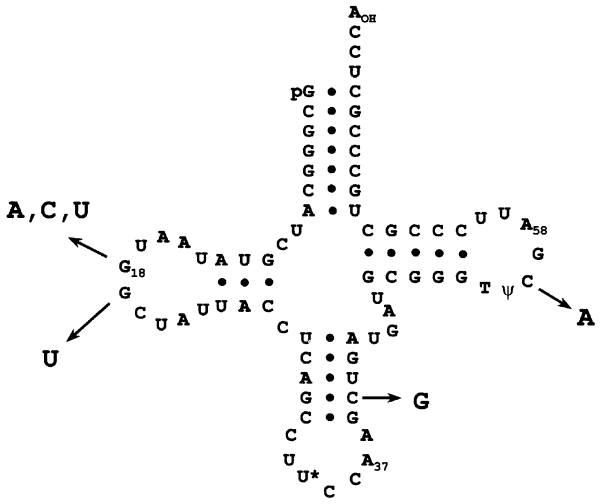

Fig. 2. Identification of *byp* mutants. Secondary structure prediction of WT tRNA$_2^{Gly}$ showing positions of *byp* mutants.

Results

We developed a genetic approach to identify features of the translational apparatus required for bypassing. The strategy was to isolate mutants of *Escherichia coli* which bypass the coding gap less efficiently using a selection based on the sucrose sensitivity conferred by the *sacB* gene from *Bacillus subtilis* (Gay *et al*., 1985).

Negative selection based on the sucrose sensitivity conferred by *sacB* has been used in Gram-negative bacteria to select for allelic exchange (Ried and Collmer, 1987; Blomfield *et al*., 1991), to select for plasmids containing inserts (Pierce *et al*., 1992), to capture insertional sequences (Gay *et al*., 1985), and to create counter-selectable transposons for use in mapping of chromosomal mutations (Lawes and Maloy, 1995). The product of *sac*B, levansucrase, releases glucose from sucrose by a transfructosylation reaction in which the byproducts are levans—large branched fructosyl polymers (Steinmetz *et al*., 1985). When expressed in *E.coli*, levansucrase is exported to the periplasmic space and appears to cause membrane fragility (Gay *et al*., 1983). We found that levansucrase requires a signal peptide at its N-terminus in order to confer sucrose sensitivity (data not shown), consistent with disruption of membrane integrity by levans.

For a selection in which efficient gene *60* expression was lethal, we created a gene *60*–*sac*B fusion with the *E.coli pho*A signal peptide coding sequence fused in-frame and upstream of gene *60*. This cassette was placed under control of an isopropyl-β-D-galactopyranoside (IPTG)-inducible tac promoter on a pBR322-based plasmid. Selection for surviving mutants was carried out in a strain which had a constitutively expressed gene *60*–*lac*Z fusion on the chromosome conferring blue color to colonies grown on plates with X-gal. Using this combination of gene fusions, we could first select for spontaneous mutants with reduced *sac*B expression and then screen on the basis of color intensity for those with lower bypassing efficiency.

We optimized selection conditions by varying sucrose and IPTG concentrations in low salt, tryptone-casamino acid broth plates until a 3- to 5-fold drop in bypassing efficiency could be detected. Using these selection conditions we screened for light blue or white colonies that survived after 24–48 h of growth. The frequency of sucrose-resistant cells was 1×10^6. Of these, one in 100 gave rise to light blue or white colonies. After confirming the color phenotype, 13 independent mutants were transformed with plasmids that allowed quantification of bypassing efficiency. Five mutants displayed a 3- to 5-fold reduction in bypassing efficiency (data not shown) and were designated *byp* mutants.

All five mutants mapped to *glyT* , the sole gene encoding tRNA$_2^{Gly}$. Sequencing PCR products amplified from each mutant provided confirmation. Four mutations are located at the universally conserved positions G18, G19 and C56

Table I. Bacterial strains

Name	Genotype	References
E.coli		
Su1675Iq	*ara Δ*(*lac-pro*) *thi recA1 F′[lacI* ^{q} *kan*^{r}*]*	Weiss *et al.* (1987)
AH108	Su1675Iq derivative *λGLZ60* (carries gene *60*–lacZ fusion)	this study
AH108*byp*G18A	AH108 derivative *glyT*(G18A)	this study
AH108*byp*G19U	AH108 derivative *glyT*(G19U)	this study
AH108*byp*C40G	AH108 derivative *glyT*(C40G)	this study
AH108*byp*C56A	AH108 derivative *glyT*(C56A)	this study
MC194	*Δ*(*lac-pro*) *thi galEΔ trpEC8 trpE91 glyT*(U34C)	gift of M.O'Connor
CSH142	*ara Δ*(*gpt-lac*)*5*	Miller (1992)
CSH142*byp*G18A	*ara Δ*(*gpt-lac*)*5 glyT*(G18A)	this study
CSH142*byp*G19U	*ara Δ*(*gpt-lac*)*5 glyT*(G19U)	this study
CSH142*byp*C40G	*ara Δ*(*gpt-lac*)5 *glyT*(C40G)	this study
CSH142*byp*C56A	*ara Δ*(*gpt-lac*)*5 glyT*(C56A)	this study
CSH142*suf*SU34C	*ara Δ*(*gpt-lac*)*5 glyT*(U34C)	this study
BW5660	*Δ*(*lac-pro*) *PK19 srbC300::Tn10 relA spoT thi supE44*	Wanner (1986)
BGS334	*lysA zgb224::Tn10 glyV55 Δ*(*tonB-trpAB*) *F′[trpA(UAG211)]*	gift of F.Pagel and E.J.Murgola
BGS347	*glyU*(*SuUAG*) *glyV55 Δ*(*tonB-trpAB*) F′[trpA(UAG211)]	gift of F.Pagel and E.J..Murgola
AH122	*ara Δ*(*gpt-lac*)*5 glyU*(*SuUAG*) *λGLZ60 argE86::Tn10*	this study
AH122*byp*G18A	*ara Δ*(*gpt-lac*)*5 glyU*(*SuUAG*) *λGLZ60 argE86::Tn10 glyT*(G18A)	this study
AH122*byp*G19U	*ara Δ*(*gpt-lac*)5 *glyU*(*SuUAG*) *λGLZ60 argE86::Tn10 glyT*(G19U)	this study
AH123	*ara Δ*(*gpt-lac*)5 *λGLZ60 argE86::Tn10*	this study
AH123*byp*G18A	*ara Δ*(*gpt-lac*)5 *λGLZ60 argE86::Tn10 glyT*(G18A)	this study
AH123*byp*G19U	*ara Δ*(*gpt-lac*)5 *λGLZ60 argE86::Tn10 glyT*(G19U)	this study
S.typhimurium		
RA1	LT2 *trpE91*	Riyasaty and Atkins (1968)
RA1*sufS601*	(see RA1) *glyT*(U34C)	Riyasaty and Atkins (1968)
RA1*sufS605*	(see RA1) *glyT*(60+U)	Riyasaty and Atkins (1968)
RA1*sufS617*	(see RA1) *glyT*(C61U)	Riyasaty and Atkins (1968)
RA1*sufS625*	(see RA1) *glyT*(C62A)	Riyasaty and Atkins (1968)
RA1*sufS627*	(see RA1) *glyT*(G1A)	Riyasaty and Atkins (1968)

(Figure 2). One mutation is in the anticodon stem at C40. Thirteen additional independent mutants were isolated: eight were at C56 and the rest were at G18. No mutations were identified in any gene besides *glyT.*

These results are intriguing because in nearly all tRNAs, G18, G19, ψ55 and C56 stabilize the elbow region by forming base pairs between the dihydrouracil (D) and ribothymidine (T) loops (Dirheimer *et al.*, 1995). G19 forms a Watson–Crick pair with C56, and G18 pairs with ψ55 through a single hydrogen bond. Importantly, the mutant versions of $tRNA_2^{Gly}$ that reduce bypassing efficiency must retain the ability to function in translation because the GGA decoding ability of $tRNA_2^{Gly}$ is required for growth of *E.coli* (Murgola and Pagel, 1980).

We chose the *byp* mutants G18A (G18 to A), G19U, C40G and C56A for further characterization. Each was transduced into a fresh background (CSH142; Table I) and bypassing efficiency and growth rates were determined. To measure bypassing efficiency, transductants were transformed with a glutathione *S*-transferase (GST)–gene *60* fusion plasmid which allows detection of proteins due to both productive and unproductive bypassing (Maldonado and Herr, 1998). Expression of these proteins was assayed by pulse–chase labeling of total protein with [^{35}S]methionine followed by separation on an SDS–polyacylamide gel (Figure 3A). All mutants bypass the coding gap at only 20–30% of wild type (WT) confirming that the *byp* phenotype is due to the mutant *gly*T alleles (Figure 3B). The growth curves and doubling times (28 min) of G18A and G19U are virtually indistinguishable from WT (data not shown). C40G and C56A also grow at nearly the same

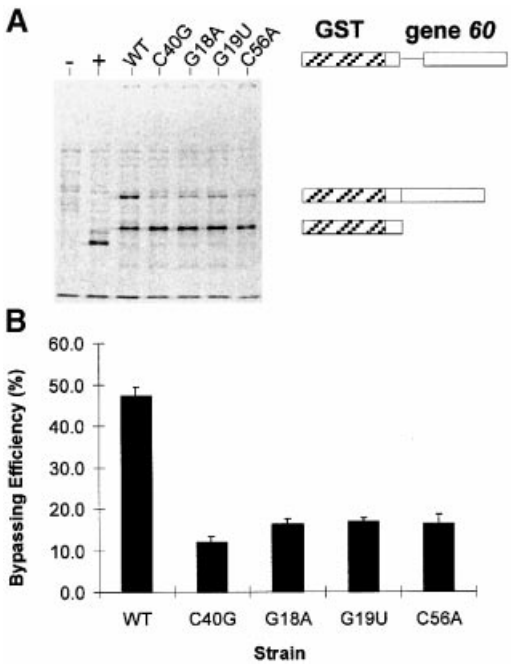

Fig. 3. Characterization of *byp* mutants. (**A**) Pulse–chase analysis of isogenic WT and *byp* mutant strains expressing a GST–gene *60* fusion. The lanes labeled '–' and '+' are negative (without the plasmid) and positive (expressing only GST) controls, respectively. The GST–gene *60* fusion and products due to productive (45.1 kDa) or unproductive bypassing (31.7 kDa) are represented schematically to the right of the autoradiograph. (**B**) The average bypassing efficiency determined from three separate experiments.

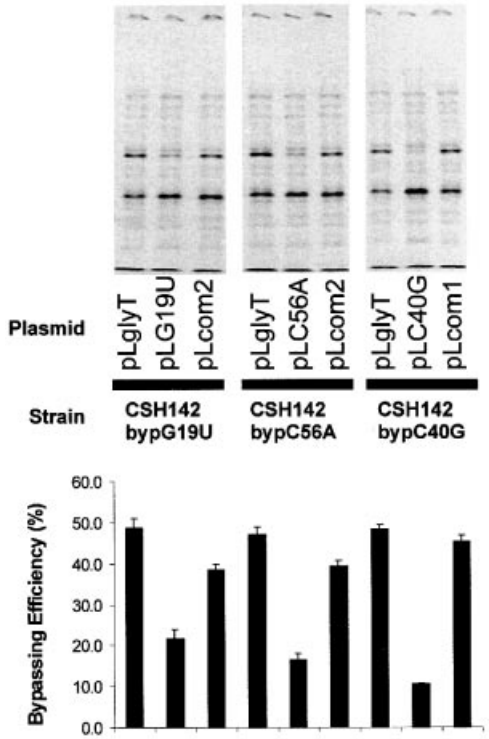

Fig. 4. *byp* mutants carrying compensatory mutations function normally in bypassing. Plasmids and the over-expressed tRNA$_2^{Gly}$ variant: pLglyT, WT; pLG19U, G19U; pLC56A, C56A; pLcom2 G19U/C56A double mutant; pLC40G, C40G; pLcom1, G30C/C40G double mutant. Top panels show pulse–chase analysis of the strains carrying both tRNA over-expression plasmids and a GST–gene *60* fusion (see Figure 3). Bottom panel shows the average bypassing efficiency determined from three separate experiments.

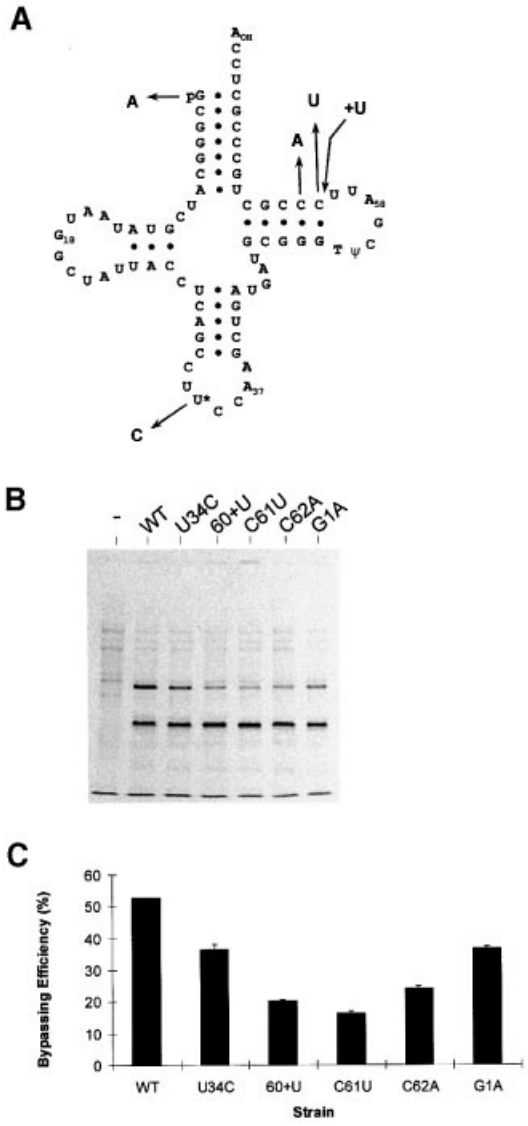

Fig. 5. *sufS* mutants and bypassing efficiency. (**A**) Secondary structure prediction of WT tRNA$_2^{Gly}$ showing positions of *sufS* mutants. (**B**) Pulse–chase analysis of *S.typhimurium trpE91* WT and *sufS* variants expressing a GST–gene *60* fusion. (**C**) The average bypassing efficiency determined from three separate experiments.

rate as WT (28–30 min) but appear to enter stationary phase at a lower density.

All of the mutants described here are predicted to disrupt base-pairing interactions within tRNA$_2^{Gly}$. To confirm that the loss of base pairing was responsible for the mutant phenotypes, compensatory mutations which restore base pairing were made in three of the mutants (Figure 4). Over-expression of tRNA$_2^{Gly}$ single mutants [G19U (pLG19U), C56A(pLC56A) or C40G(pLC40G)] does not overcome the defect in bypassing in strains carrying a chromosomal *byp* mutation. In contrast, double mutants carrying the compensatory changes correct the defect in bypassing. G19U/C56A(pLcom2) restores bypassing efficiency to ~80% of WT in both G19U and C56A backgrounds. (The lack of complete restoration may reflect either a residual defect in bypassing or competition with the chromosomal *byp* mutant.) G30C/C40G(pLcom1) restores bypassing efficiency to ~100% of WT in a C40G background. These results show that the structural integrity of the tRNA is critical for bypassing.

There are mutants of *Salmonella typhimurium* in *gly*T that promote –1 frameshifting at the sequence G GGA (Riyasaty and Atkins, 1968; O'Mahony *et al*., 1989a; Pagel *et al*., 1992). These recessive alleles, called *suf*S for suppressor of frameshift mutation, include the mutations U34C, 60+U (an extra U between U59 and U60), C61U, C62A and G1A (Figure 5A). We tested these mutations for altered bypassing efficiency (Figure 5B). U34C and G1A reduce bypassing efficiency to 70% of WT while 60+U, C61U and C62A reduce bypassing efficiency to nearly the same extent as *byp* mutants (30–40% of WT) (Figure 5C). Those mutants with T-stem or T-loop defects (60+U, C61U, C62A) may be analogous to the *byp* mutants which disrupt the elbow region. Previous work showed 60+U and C61U variants are present at low abundance and aminoacylated poorly (O'Mahony *et al*., 1989b). This suggests that aminoacyl-tRNA$_2^{Gly}$ levels may influence bypassing efficiency.

To determine whether aminoacyl-tRNA$_2^{Gly}$ levels are correlated with the decrease in bypassing, we measured tRNA abundance by Northern analysis of tRNA preparations purified and separated under conditions which preserve the aminoacyl-tRNA bond and separate aminoacyl-tRNA from deacyl-tRNA. A sample subjected to base-treatment (which hydrolyzes the aminoacyl bond) is analyzed alongside each untreated sample to provide a size marker for the faster migrating deacyl-tRNA. Our

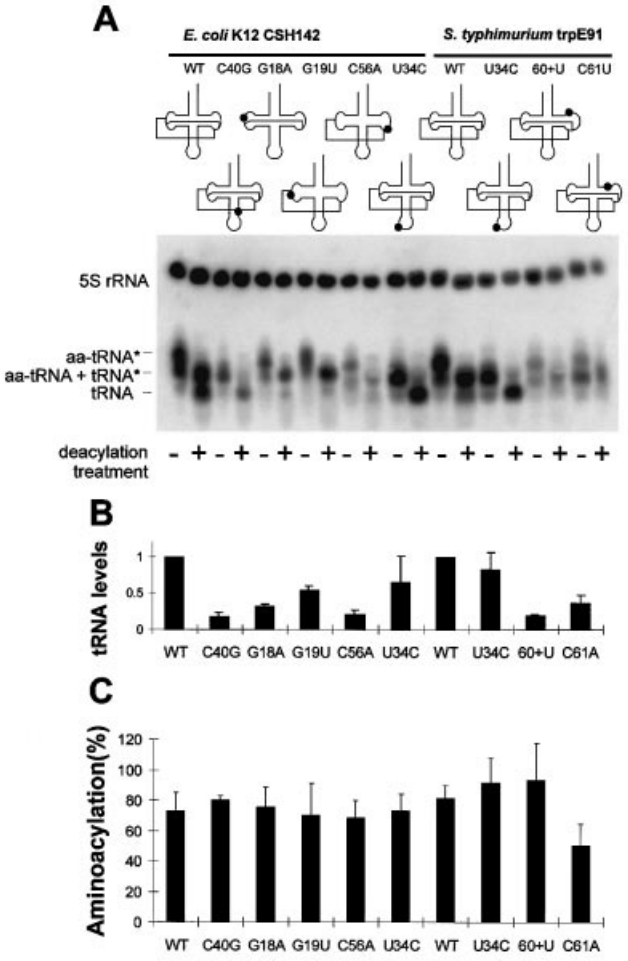

Fig. 6. Aminoacyl-tRNA$_2^{Gly}$ levels in *byp* and *sufS* mutants. (**A**) Northern blot analysis of total tRNA purified and separated under acidic conditions. Strains: for complete genotypes see Table I. Abbreviations: aa-tRNA*, modified aminoacyl-tRNA$_2^{Gly}$; aa-tRNA, unmodified aminoacyl-tRNA$_2^{Gly}$; tRNA*, modified deacyl-tRNA$_2^{Gly}$; tRNA, unmodified deacyl-tRNA$_2^{Gly}$. Deacylation treatment: '–', untreated sample; '+' treated with Tris pH 9.0 prior to analysis. An oligonucleotide complementary to nucleotides 27–54 of tRNA$_2^{Gly}$ served as the probe. (**B**) The average tRNA levels in each strain (determined from untreated samples) from three separate experiments normalized to the appropriate WT control. (**C**) The average estimated percentage of tRNA$_2^{Gly}$ which is aminoacylated.

analysis of tRNA$_2^{Gly}$ levels in WT, G18A, G19U, C56A, 60+U and C61U preparations reveal two species of aminoacyl-tRNA$_2^{Gly}$ with different electrophoretic mobilities (Figure 6A). C40G and U34C preparations, by contrast, show only the faster migrating form of aminoacyl-tRNA$_2^{Gly}$. The most likely explanation for the two species is the presence or absence of the modified nucleotide U* at position 34. This is consistent with U34C showing a single species and with a partial characterization of U* determined during the sequencing of tRNA$_2^{Gly}$ (Roberts and Carbon, 1975). This characterization showed U* was similar to 2-thio-5(methylaminomethyl) uridylic acid and that U* had a lower electrophoretic mobility than uridine. Furthermore, the authors noted in some preparations of tRNA, only 70% of tRNA$_2^{Gly}$ carries U*, which is consistent with the ratios of the two products we see in most samples. The observation that C40G preparations lack U* suggests the stability of the anticodon stem may be important for modification.

Determining aminoacyl-tRNA levels is complicated by the U* modification because deacylated modified tRNA$_2^{Gly}$ co-migrates with unmodified aminoacyl-tRNA$_2^{Gly}$. Therefore, to determine aminoacyl-tRNA levels, we first measured total tRNA levels and then estimated the percentage which was aminoacylated.

Total tRNA levels were determined by quantifying the amount of hybridization to tRNA$_2^{Gly}$ in each sample (modified and unmodified), correcting for loading differences using the amount of hybridization to 5S rRNA, and then normalizing the amount of each mutant tRNA to the wild-type control (Figure 6B). From this analysis, C40G, C56A and 60+U are present at <20% of WT levels. G18A, G19U and C61U are present at 30–50% of WT levels. U34C (which was assayed in both *S.typhimurium* and *E.coli*) showed a substantial amount of variability, but in some assays was as abundant as WT.

The percentage of aminoacyl-tRNA$_2^{Gly}$ in WT, G18A, G19U, C56A, 60+U and C61U preparations was estimated by comparing amounts of modified aminoacyl-tRNA (Figure 6A, '–' lanes) to base-treated modified deacyl-tRNA (Figure 6A, '+' lanes). The unmodified variants (C40G and U34C) were analyzed in a similar fashion. The results (Figure 6C) suggest the percentage of tRNA$_2^{Gly}$ which is aminoacylated is similar for both mutants and WT, and indicates that total tRNA levels are a reasonable estimate for aminoacyl-tRNA levels. The variability in aminoacyl-tRNA levels alone does not seem to account for the decrease in bypassing efficiency: C56A is 3-fold less abundant than G19U, yet both have the same decrease in bypassing efficiency.

We investigated whether the decoding ability of the mutants is correlated with the decrease in bypassing efficiency. Decoding efficiency of tRNA$_2^{Gly}$ variants with a 3′AUC anticodon was measured using an amber suppression assay. Expression vectors were constructed in which transcription of amber suppressor tRNA$_2^{Gly}$ variants was controlled by a temperature-sensitive λ repressor (Figure 7A). Amber suppression was monitored using a protA-cat-lacZ construct interrupted by a UAG codon and normalized to a control with a sense codon replacing the UAG. After 1 h of growth at 40°C to ensure steady-state levels of suppressor tRNA, *lacZ* expression was induced. At the end of induction, total tRNA was purified and separated using conditions which preserve the aminoacyl bond. The samples were then subjected to Northern analysis using a probe (Figure 7B) and hybridization conditions under which only amber suppressor tRNA$_2^{Gly}$ was detected (Figure 7C).

Northern analysis of both base-treated and untreated C56A reveals a slower migrating product which may reflect a processing defect (Figure 7C). This is consistent with a loss of recognition by RNaseP which makes specific contacts with the T-stem and loop of pre-tRNA (Svard and Kirsebom, 1993; Gaur *et al*., 1996). Alternatively, it may reflect a polyadenylated degradation intermediate (Li *et al*., 1998). The reduced mutant tRNA levels seen both here and in Figure 7 may indicate an additional processing defect: complete degradation during 3′ processing by 3′→5′ exonucleases (Li and Deutscher, 1996).

Decoding efficiency was calculated by correcting the normalized amber suppression levels by the normalized aminoacyl-tRNA$_2^{Gly}$ (SuUAG) levels (Figure 7D). The

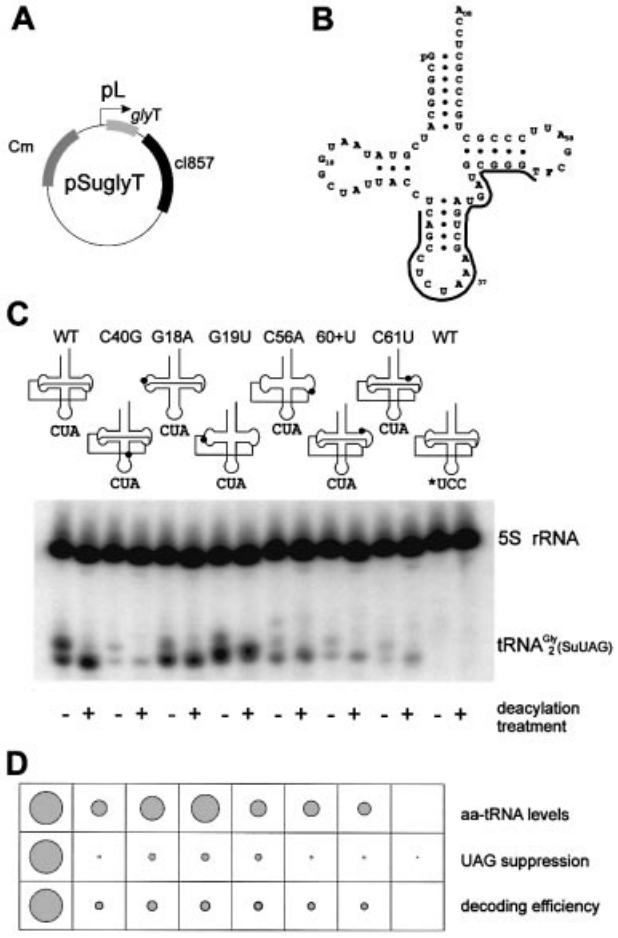

Fig. 7. Decoding efficiency of tRNA$_2^{Gly}$ mutants. (**A**) Expression construct. (**B**) Secondary structure prediction of tRNA$_2^{Gly}$ amber suppressor [tRNA$_2^{Gly}$ (SuUAG)] variants. The bold line represents the oligonucleotide probe used to detect tRNA$_2^{Gly}$ (SuUAG) variants. (**C**) Northern analysis of total tRNA purified and separated under acidic conditions from WT strains over-expressing tRNA$_2^{Gly}$ (SuUAG) variants or WT tRNA$_2^{Gly}$. Deacylation treatment: see Figure 6. (**D**) Decoding efficiency determination. The area of the each circle corresponds to the normalized activity or concentration of the corresponding tRNA. Estimates represent the average of three separate experiments.

results show that all tRNA$_2^{Gly}$ variants that reduce bypassing are 10- to 20-fold down in decoding efficiency.

The observation that these tRNA$_2^{Gly}$ mutants are reduced in both decoding and bypassing efficiency can be explained by two models. In the first model, the drop in tRNA$_2^{Gly}$ decoding efficiency starves ribosomes at GGA codons. As a result, ribosomes stalled just before the take-off site GGA are diverted from bypassing by competing events such as tRNA$_1^{Gly}$ near-cognate decoding. [tRNA$_1^{Gly}$ near-cognate decoding has been invoked to account for the –1 frameshift activity of 60+U and C61U (O'Connor, 1998; Qian *et al*., 1998). Ribosomes which shift –1 at the take-off site would terminate at a UAG within the coding gap. tRNA$_3^{Gly}$ (anticodon = 3′CCG) has been shown to read GGA *in vitro* under conditions of no competition, but competes poorly with tRNA$_2^{Gly}$ or tRNA$_1^{Gly}$ for GGA codons (Samuelsson *et al*., 1983).] In the second model, despite the decrease in decoding efficiency, tRNA$_2^{Gly}$ still decodes the take-off site GGA and a reduction in stability in the P-site leads to a decrease in landing efficiency.

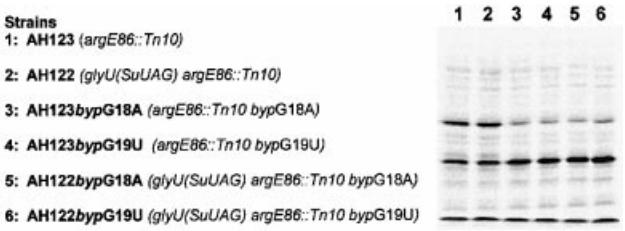

Fig. 8. tRNA$_1^{Gly}$ and the *byp* mutant phenotype. Strains and relevant genotypes are listed to the left (see also Table I). Pulse–chase analysis of the strains expressing a GST–gene *60* is shown to the right.

To distinguish between these two models, we first tested whether the reduction in bypassing was due to tRNA$_1^{Gly}$ near-cognate decoding. tRNA$_1^{Gly}$ (encoded by *glyU*) has a 3′CCC anticodon and decodes primarily GGG codons. A *glyU*(SuUAG) strain, which expresses an amber suppressor variant of tRNA$_1^{Gly}$ (anticodon 3′CUA), was transduced to tetracycline resistance with P1 lysates grown on *byp* mutants carrying a Tn*10* linked to *gly*T (argE86::Tn10). Mutant tRNA$_2^{Gly}$ must have sufficient activity to decode all GGA and GGG codons for the double mutants to be viable. Transductional crosses with C40G and C56A mutant showed that these alleles do not meet this requirement (data not shown). No double mutants were obtained even though argE86::Tn10 is 50% linked to *gly*T. On the other hand, G18A-*gly*U(SuUAG) and G19U-*gly*U-(SuUAG) double mutants were readily obtained. Bypassing efficiency in these strains remains 3- to 5-fold less than WT, showing that tRNA$_1^{Gly}$ is not necessary for the *byp* phenotype of these mutants (Figure 8).

Additional evidence discounts the starvation-dependent model. This model predicts that over-expression of *byp* mutants may partially suppress the bypassing defects associated with a chromosomal *byp* mutant. The results from Figure 4 show no indication that over-expression of G19U, C56A or C40G increases bypassing in a *byp* mutant strain. The starvation-dependent model also predicts that over-expression of *byp* mutants will have no effect on bypassing in a WT cell. We tested the second prediction by monitoring bypassing in WT cells over-expressing different tRNA$_2^{Gly}$ variants (data not shown). Over-expression of C40G, G18A or G19U reduces bypassing by 20–30%, arguing against the starvation-dependent model. Instead, these results support a model in which tRNA$_2^{Gly}$ mutants directly interfere with the bypassing mechanism in the P-site.

Discussion

The decoding properties of peptidyl-tRNA$_2^{Gly}$ are critical for each stage of gene *60* bypassing. Destabilization of peptidyl-tRNA$_2^{Gly}$ pairing with the take-off site GGA is required for bypassing initiation. Peptidyl-tRNA$_2^{Gly}$ probing of the coding gap for a cognate interaction is required during scanning, and peptidyl-tRNA$_2^{Gly}$ pairing with the landing site GGA is necessary for resumption of decoding in the correct downstream reading frame. The *glyT* mutants described here may disrupt bypassing during either take-off, scanning or landing. The observation that each mutant pairs inefficiently with its cognate codon in the A-site suggests that the defect occurs after take-off.

In one model for reduced bypassing, increased dissoci-

ation of mutant peptidyl-tRNA$_2^{Gly}$ from cognate codons diminishes recognition of the landing site GGA during scanning. Ribosomes which fail to form a stable interaction with the landing site either resume translation at random non-cognate sites or dissociate from the mRNA completely. In a second model, weakened tRNA–ribosome contacts in the P site during scanning lead to high rates of peptidyl-tRNA dissociation from the ribosome. Non-cognate landing and mRNA or peptidyl-tRNA$_2^{Gly}$ dissociation from the ribosome may all occur during WT bypassing—only 50% of ribosomes poised at the take-off site bypass productively. Experiments to determine the fate of ribosomes which fail to bypass in WT and mutant *glyT* strains are underway.

Mutations in the anticodon stem and elbow region of tRNA$_2^{Gly}$ show nearly identical decreases in bypassing efficiency and decoding ability. This poses the question of how these two regions of tRNA act to stabilize codon–anticodon pairing. To address this question, we examined the predicted structural consequences of the mutants and then looked at the role structure may play in stabilizing codon–anticodon interactions.

Structural consequences of mutations

Three of the seven tRNA$_2^{Gly}$ mutants that display a *byp* phenotype are predicted to increase the flexibility of the elbow region by altering the highly conserved base pairs between the D- and T-loops (Dirheimer *et al*., 1995). G19U and C56A disrupt the G19•C56 Watson–Crick base pair at the corner of the elbow which locks the loops together. Rare, naturally occurring examples of the disrupted pairs (U19•C56 or G19•A56) exist (Sprinzl *et al*., 1998) but the properties of these tRNA have not been investigated. Mutations at G18 interfere with the other hydrogen bonding contact between the loops (N2 of G18 to O4 of Ψ55) and may reduce the stacking energy gained by G18 intercalation between G57 and m^{1}A58.

Three of the remaining mutants are predicted to increase the flexibility of the elbow region by altering the T-loop. Two of these may affect a stabilizing hydrogen bond between phosphate 60 (P60) and N4 of C61. The extra U in 60+U may distort the backbone and move P60 out of hydrogen bonding range with N4. This type of disruption has been reported for the addition of an A to the T-loop of tRNA^{Asp} (Romby *et al*., 1987). Interestingly, addition of the A also destabilizes the interaction between the D- and T-loops as shown by an increase of C56 to chemical modification. C61U disrupts the P60–N4 hydrogen bond by virtue of eliminating N4. Romby *et al*. (1987) noted, in a C61U variant of tRNA^{Asp}, that P60 became highly accessible to chemical modification suggesting the other hydrogen bond it makes (to 02′ of A58) may also be weakened. The third mutation (C62A) creates a G–A mismatch in the T-stem which must distort or destabilize G53•C61, perhaps also affecting the P60–N4 hydrogen bond. Thus, all of the *byp* mutations in the T-stem–loop may increase the T-loop flexibility and potentially alter its interaction with the D-loop.

The lone *byp* mutation in the anticodon stem (C40G) creates a G–G mismatch in a region defined genetically as the extended anticodon (Yarus, 1982). The work of Yarus and colleagues indicates that for each possible 3′ nucleotide in the anticodon (which pairs with the first base of the codon) there is an optimal sequence for certain nucleotides in the anticodon loop and for the first two base pairs of the anticodon stem (31•39 and 30•40) (Yarus *et al*., 1986a,b). Changing these positions or base pairs from the optimum reduces decoding efficiency. Structurally, the G–G pair in tRNA$_2^{Gly}$ may destabilize the stem and alter its stacking interactions with bases in the anticodon loop.

tRNA structure and stability of codon–anticodon pairing

The preceding discussion suggests that each of the tRNA$_2^{Gly}$ mutants reduces the structural rigidity of the tRNA. The immediate effects of this increased flexibility may be different for mutants in the elbow region versus mutants in the anticodon stem, but ultimately the loss of stability results in diminished codon–anticodon pairing in both the A- and P-sites of the ribosome. The coincident loss of tRNA structure and decoding ability suggests the mutations may interfere with a dynamic interaction between the tRNA and ribosome which stabilizes cognate pairing.

The contribution that ribosomes make to codon–anticodon stability is substantial. Estimates indicate that cognate interactions in the A-site of the ribosome are stabilized between 10- and 100-fold (at 20–25°C) over both non-cognate interactions in the A-site and cognate interactions in solution (Grosjean *et al*., 1976; Karim and Thompson, 1986; Pape *et al*., 1998). Chemical protection studies with A-site tRNA or anticodon loop analogues suggest that the majority of the contacts are between the anticodon stem–loop and the decoding center of 16S rRNA (Green and Noller, 1997). These same studies indicate P-site tRNA also makes extensive contacts with 16S rRNA suggesting ribosome-mediated stabilization continues in the P-site. Contacts between 23S rRNA and tRNA appear to be almost exclusively with the CCA end (Green and Noller, 1997). Thus, with respect to rRNA contacts, the main ribosome–tRNA interactions are at the extremities of the tRNA.

A conformational adjustment by tRNA may trigger the ribosome to stabilize cognate codon–anticodon pairing. Evidence for a conformational change in tRNA during the decoding step comes from several sources. One source is genetic studies which examined the consequences (with respect to decoding) of altering the D-anticodon domain of tRNA. Mutations affecting the 12-23-9 triple base pair allow normally forbidden third position wobble pairs during the decoding step (Hirsh, 1971; Smith and Yarus, 1989). Similarly, mutations at the 27–43 pair (Schultz and Yarus, 1994) allow first position wobble pairs. Together, these results suggest the conformation of the D-anticodon domain of tRNA influences dissociation rates from the A-site (Yarus and Smith, 1995).

Additional support for a conformational change in tRNA upon codon–anticodon pairing comes from fluorescence studies which showed that ternary complex binding to a cognate codon in the A-site induces a conformational change in the D-loop (Rodnina *et al*., 1994). A striking parallel observation comes from comparison of the crystal structure of tRNA^{Phe} (of a monomer) with the crystal structure of tRNA^{Asp} [of a dimer of monomers bound by their nearly self-complementary anticodon loops (GUC)] (Moras *et al*., 1980; Westhof *et al*., 1985). The G19•C56

base pair does not form in tRNA^{Asp} in stark contrast to tRNA^{Phe}. This lack of pairing correlates with increased flexibility in the elbow region and increased rigidity in the anticodon stem. The crystal structure, however, may not tell the whole story. The fluorescence studies suggest that the conformation of the D-loop is at least partially restored following release of the tRNA into the A-site (Rodnina *et al*., 1994). In agreement with this conclusion, the results presented here show that stability of the elbow contributes to codon–anticodon stability.

Given this view of the interplay between the ribosome and tRNA, it is not hard to imagine how mutants of the elbow region and anticodon stem destabilize codon–anticodon pairing. The C40G mutation may directly interfere with 30S subunit contacts to the anticodon stem region. Alternatively, it may disrupt a conformational change in the tRNA which improves tRNA–ribosome contacts. The flexibility found in mutants of the elbow region may destabilize tRNA–30S subunit contacts by altering the D-anticodon domain or by altering intersubunit contacts. A final possibility, applicable to both types of mutants, takes into account the low but significant rates of WT peptidyl-tRNA dissociation and re-pairing. Evidence for this comes from the 'stop-hopping' observed during translation of the sequence CUU UAG CUA. Peptidyl-tRNA^{Leu} detaches from the CUU, bypasses the stop codon, and re-pairs at the CUA at an efficiency of 1% (Weiss *et al*., 1987). The predicted increased flexibility found in mutants of the elbow region and anticodon stem of tRNA$_2^{Gly}$ may lower the efficiency of re-pairing (whether at ordinary GGA codons or at the landing site GGA) by causing misalignment of the D-anticodon domain with respect to the P-site codon.

The mutations in tRNA$_2^{Gly}$ described here add to a collection of mutants which affect the stability of peptidyl-tRNA pairing with mRNA. Not surprisingly, tRNA mutations which alter the anticodon loop have significant effects, that is, addition of an extra nucleotide to the anticodon of tRNA$_1^{Val}$ allows this tRNA to detach and re-pair at matching valine codons at high frequency (O'Connor *et al*., 1989). Mutations which influence peptidyl-tRNA decoding have also been identified in nucleotides comprising the decoding domain of 16S rRNA (530 loop, helix 34 and 1400–1500 region) (O'Connor *et al*., 1997). Finally, mutations in ribosomal protein L9 enhance both gene *60* bypassing and stop-hopping (Herbst *et al*., 1994). The continued exploitation of genetic systems in which peptidyl-tRNA detachment and re-pairing occurs will undoubtedly yield additional insights into how the translational apparatus maintains peptidyl-tRNA–mRNA pairing.

The importance of the L structure of tRNA is implicit in its extraordinary conservation in all organisms. The three dimensional structure of the functional sites of the ribosome maintains a selection for tRNA molecules and translation factors that conform to certain structural specifications. The tRNA$_2^{Gly}$ mutants described here, especially the mutants of the elbow region, indicate that one functional role of the rigidity of the L structure is to ensure stable codon–anticodon interactions.

Materials and methods

Plasmid constructions

All plasmid constructions were confirmed by DNA sequencing on automated sequencing machines (ABI-100).

Sucrose selection plasmid. The *phoA*-gene *60-sacB* plasmid (GSB228×3) was constructed in three steps. (i) *SacB* was amplified by PCR using a sense primer with an embedded *Apa*I site (GCTTGGGCCCATCTTCTAAA GCTAACATCAAAAAGTTTGCAAAACAAGC) and an anti-sense primer with an embedded *Sal*I site (GCGCGCGTCGACTTATTTGTTAACTGTTAATTGTCCTTGTTC) from a *sacB* expression vector (unpublished data) in which the *Hin*dIII site [starting at nt 1798 (DDBJ/EMBL/GenBank accession No. X02730)] and the *Kpn*I site (starting at 1521) had been mutated to CAGCTT and GGTATC, respectively. This PCR fragment was cloned into the *Apa*I and *Sal*I sites of a gene *60–lacZ* expression vector (GLZ30; Maldonado and Herr, 1998) in which the *lacZ* fusion is controlled by an IPTG-inducible tac promoter. (ii) The ribosome binding site (RBS) and first 43 codons of *E.coli phoA* was amplified and cloned into the *Xba*I and *Hin*dIII sites using a sense primer with an embedded *Xba*I site (CATGTCTAGATTAATTGGAGAAAATAAAATGAAACAAAGCA CTATTGCACTGG) and an anti-sense primer with an embedded *Hin*dIII site (CTAGAAGCTTACCGCCGGGTGCAGTAATATCGCCCTG). And (iii), the first 48 codons of gene *60* was amplified using a sense primer with an embedded *Hin*dIII site (GATCAAGCTTATGAAATTTGTAAAAATTGATTCTTC) and an anti-sense primer with an embedded *Apa*I site (GGTTAGGGCCCCCTAATCCATCGTGATCTGCGTCTG) and cloned between *phoA* and *sacB*. A control with a 3-fold reduction in bypassing [amplified from (BX5b) (Weiss *et al*., 1990)] was also made (GSB228×5b).

tRNA over-expression plasmids. The *Xba*I–*Sal*I fragment of pACYC184 (Chang and Cohen, 1978) was replaced with a sequence which eliminates the *Xba*I site and introduces the bacteriophage λ 6S terminator and a *Kpn*I site upstream of *Sal*I. The 3.4 kb *Kpn*I–*Sal*I fragment from GLZ30 was subsequently cloned into this vector to create GLZ30/ACYC. The tac promoter, flanked by *Kpn*I and *Xba*I sites, was then replaced with the pL region of bacteriophage λ amplified by PCR using primers with embedded *Xba*I and *Kpn*I sites (GATCTCTAGAGCTGATGTGCTCAGTATCACCGCCAGTGG and GATCGGTACCTTGCCT CACGATCGCCCCCAAAACACATAACC, respectively) to create pLEX1. All tRNA^{Gly} genes were cloned into pLEX1 using downstream *Hin*dIII and *Sal*I sites. *glyT* PCR products were amplified from *E.coli* or *S.typhimurium* strains using a sense primer with an embedded *Hin*dIII site located upstream of *glyT* in *tyrU* (GATCAAGCTTCTTCGAATCCTTCCCCCACCACC) and an anti-sense primer with an embedded *Sal*I site located downstream in *thrT* (GATCGTCGACGACCTCACCCTTACCAAGGGTGCG). pLcom1 and pLcom2 (Figure 4) were made using a two-step PCR strategy and internal primers which allowed the appropriate compensatory mutation to be made. *E.coli glyU* was amplified using primers with embedded *Hin*dIII and *Sal*I sites (GATCAAGCTT AAAATGCTGATGGCGAATAATCGCAGTC and GATCGGGCCCTTGTTAAAAAGCGTAGATAA CCACTTATTTAAG, respectively).

To make pSuGlyT plasmids (Figure 7), a temperature-sensitive bacteriophage λ cI allele (cI857) was amplified using a primer with an overhang carrying an embedded *Sal*I site, the *lac*I^q promoter, and a synthetic RBS (GATCGTCGACACCATCGAATGGTGCAAAACCTTTCGCGGTATGGCATGATAGCGCCCGGAAGAGAGTCAATTCAGGAGAATCGTATGAGCACAAAAAAGAAACCATTAACACAAGAGCAGC) and a primer with an embedded *Eag*I site (GATCCGGCCGTGCCGATCAGCCAAACGTCTCTTCAGGCCACTG). This was cloned into pLEX1 using *Sal*I and *Eag*I sites to create pLEX2. Amber suppressor derivatives of *glyT* alleles were amplified using a two-step PCR strategy and cloned into the *Xba*I and *Sal*I sites of pLEX2. The outside primers were the same as detailed above except the primer in *tyrU* carried an embedded *Xba*I site. The internal primers changed the anticodon of *glyT* to 3′AUC.

ProtA-cat-lacZ expression plasmids for the amber suppression assays were constructed by amplifying the RBS and coding sequence of protA-cat from 4p112 (Weiss *et al*., 1987) by PCR and subcloning it into the *Xba*I and *Hin*dIII sites of GLZ30 creating GLZ69. An oligonucleotide insert which separated the protA-cat and lacZ open reading frames by a UAG codon was then cloned between *Hin*dIII and *Apa*I sites creating GLZ96. A test construct with a CAG sense codon replacing the UAG codon was also made: GLZ95.

Genetic experiments

All genetic manipulations were carried out essentially as described (Miller, 1972, 1992). The genotypes of strains used are listed in Table I.

The *E.coli* strain for the selection (which carries a gene *60–lacZ* fusion on the chromosome) was created in three steps. First, the promoter of the plasmid GLZ16 (Maldonado and Herr, 1998) was replaced with

the constitutive σ70 *E.coli* consensus promoter (Watson *et al*., 1983) to create GLZ60. Secondly, this plasmid was recombined with λRS45, as described by Simons *et al*. (1987), to create λGLZ60. Finally, a Su1675I^q λGLZ60 lysogen was made and designated AH108.

Selection conditions where a 3-fold decrease in bypassing efficiency could be detected were determined by monitoring the survival of 10^3 Su1675I^q [GSB228×5b] cells against a background of 10^8 AH108[GSB228×3] cells on TCB plates (10 g tryptone, 5 g casamino acids, 17 g Bacto-agar, 0.2% glucose, 40 μg/ml X-gal, 1× A-salts per liter) with variable concentrations of IPTG and sucrose. Plates with 10–20 μm IPTG and 2.5% sucrose proved to be optimal.

Identification of mutants. Aliquots (0.1 ml) of 8 h 2 ml Luria–Bertani (LB) cultures were plated on selection plates and incubated for 24–48 h. Light blue or white colonies were picked and streaked on LB X-gal plates to confirm the color phenotype. To test if bypassing was reduced, putative mutants were transformed with compatible plasmids which allowed bypassing to be quantified.

Mutants displaying a significant reduction in bypassing efficiency were mapped and sequenced in seven steps. (i) AH108*byp*[GSB228×3] strains were cured of the selection plasmid using courmermycin (Danilevskaya and Gragerov, 1980). (ii) AH108*byp* F$^-$ phenocopies were mated with BW5660 to introduce *recA*$^+$ linked to *srbC300::Tn10*. (iii) The resulting kan^r tet^r UV^r exconjugants were transduced to sorbital utilization and tet sensitivity. (iv) Matings of F$^-$ phenocopies of the resulting transductants to tet^r Hfr mapping strains (Singer *et al*., 1989), were used to localize the mutants to the region between 89 and 6 min (clockwise) on the *E.coli* chromosome. (v) Transductional crosses with strains having Tn*10*'s near genes involved in translation in the localized region (Singer *et al*., 1989) were used to map the mutations to the *tufB* operon. (The mutants were 50% linked to ArgE86::Tn*10* and 70% linked to thi-39::Tn*10*.) (vi) Complementation performed using previously described *tufB* expression plasmids suggested that the mutations were in glyT (Van Delft *et al*., 1987). (vii) PCR products were amplified and sequenced using primers upstream of *glyT* in *tyrU* and downstream in *thrT*. For further characterization, the *byp* mutants were moved into CSH142 using P1 transduction and a linked Tn*10* (*argE86::Tn10*). The resulting transductants were then transduced to arginine prototrophy to remove the Tn*10*.

Note on the sacB selection. One limitation of the *sacB* selection system is that mutants which reduce both levansucrase production and growth rate may not survive. Mutants appear to survive only if they increase the ratio of growth rate/levan synthesis beyond a certain threshold. This may explain why 60+U, C61U and C62A were not isolated even though these reduce bypassing to levels comparable to *byp* mutants.

$tRNA_I^{Gly}$ and the byp mutant phentype. AH122 and *byp* mutant derivatives were constructed in three steps. (i) A P1 lysate grown on BGS334 was used to transduce a CSH142 λGLZ60 lysogen to tet^r and *lysA*. (ii) This strain was transduced to lysine prototrophy and *glyU*(*SuUAG*) with a P1 lysate grown on BGS347. Presence of *glyU*(*SuUAG*) was confirmed by transducing BGS334 to lysine prototropy and testing for suppression of trpA(UAG211). (iii) This strain was transduced to tet^r using P1 lysates grown on *byp* mutants carrying argE86::Tn*10*. A CSH142 λGLZ60 lysogen was transduced as a control in these experiments creating AH123.

Bypassing efficiency assays

Bypassing efficiency measurements were performed essentially as described (Maldonado and Herr, 1998) using [^{35}S]methionine pulse–chase analysis. Cells carrying a GST–gene *60* expression plasmid were grown to mid-log phase in MOPS–glucose (Neidhardt *et al*., 1974) containing all amino acids (150 μg/ml each) except methionine. Expression was induced with IPTG for 8 min, after which total protein was labeled by the addition of 7.5 μCi [^{35}S]methionine. After a 1 min labeling period, the radioactivity was chased by addition of an excess of cold methionine for 3 min. Following pulse–chase labeling, total protein in each sample was separated on a 12% Tris–glycine SDS polyacylamide and visualized with a Molecular Dynamics PhosphorImager. Efficiency estimates represent the amount of bypassing product divided by the total protein synthesized from the GST–gene *60* fusion (bypassing product + termination product). All efficiency estimates were determined by averaging at least three independent assays and were corrected for differences in methionine content between the bypassing product and termination product.

Aminoacyl-tRNA purification and detection

Whole aminoacyl-tRNA was purified as described (Varshney *et al*., 1991; Bourdeau *et al*., 1998), separated on an acidic denaturing 6% polyacrylamide gel, blotted to a Zeta-probe membrane (Bio-Rad) and probed using ^{32}P-end labeled oligonucleotide probes complementary to nucleotides 27–54 of $tRNA_2^{Gly}$ or $tRNA_2^{Gly}$ (SuUAG). 5S rRNA was simultaneously probed using a ^{32}P-end labeled oligonucleotide complementary to nucleotides 30–60. Loading differences between the samples were corrected for by normalizing $tRNA_2^{Gly}$ levels to 5S rRNA levels. Mutant tRNA levels were then normalized relative to WT levels. Three separate preparations of tRNA were assayed for each estimate.

Decoding efficiency estimates

O/N 37°C cultures of AH108 strains carrying $tRNA_2^{Gly}$ (SuUAG) overexpression plasmids and GLZ96 (UAG containing test construct) or GLZ95 (control construct; see above) were diluted 1:50 and grown for 1 h at 40°C. *LacZ* expression was then induced with 2 mM IPTG for an additional 90 min of growth before β-galactosidase activity was assayed (Miller, 1972; Maldonado and Herr, 1998) and whole tRNA was purified. β-galactosidase levels from test constructs were corrected by levels from control constructs to give an amber suppression efficiency for each $tRNA_2^{Gly}$ (SuUAG) variant. Decoding efficiency estimates were made by correcting the amber suppression efficiency by the levels of aminoacyl-$tRNA_2^{Gly}$ (SuUAG) in each sample. Estimates represent the average of three independent measurements.

Acknowledgements

We thank Steve Alam, Mike Howard and Doug Bucklin for critical reading of the manuscript. We thank Fran Pagel and Manny Murgola for bacterial strains BGS334 and BGS347. We also thank Alan Collmer for providing a *sacB* expression vector. Finally, we are grateful to Michael O'Connor for both bacterial strains and helpful discussions. This work was supported by a grants (to J.F.A.) from NIH (GM48152), and (to R.F.G.) from DOE (DE-FG03-99ER62732/A000). A.J.H. is supported by an NIH training grant (#5T32GM07464-24).

References

Adamski,F.M., Atkins,J.F. and Gesteland,R.F. (1996) Ribosomal protein L9 interactions with 23S rRNA: the use of a translational bypass assay to study the effect of amino acid substitutions. *J. Mol. Biol.*, **261**, 357–371.

Atkins,J.F. and Gesteland,R.F. (1995) Discontinuous triplet decoding with or without re-pairing by peptidyl-tRNA. In Soll,D. and RajBhandary,U.L. (eds), *tRNA: Structure, Biosynthesis and Function*. ASM press, Washington, DC, pp. 471–490.

Blomfield,I.C., Vaughn,V., Rest,R.F. and Eisenstein,B.I. (1991) Allelic exchange in *Escherichia coli* using the *Bacillus subtilis sacB* gene and a temperature-sensitive pSC101 replicon. *Mol. Microbiol.*, **5**, 1447–1457.

Bourdeau,V., Steinberg,S.V., Ferbeyre,G., Emond,R., Cermakian,N. and Cedergren,R. (1998) Amber suppression in *Escherichia coli* by unusual mitochondria-like transfer RNAs. *Proc. Natl Acad. Sci. USA*, **95**, 1375–1380.

Brierley,I. (1995) Ribosomal frameshifting on viral RNAs. *J. Gen. Virol.*, **76**, 1885–1892.

Chang,A.C. and Cohen,S.N. (1978) Construction and characterization of amplifiable multicopy DNA cloning vehicles derived from the P15A cryptic miniplasmid. *J. Bacteriol.*, **134**, 1141–1156.

Chittum,H.S., Lane,W.S., Carlson,B.A., Roller,P.P., Lung,F.D., Lee,B.J. and Hatfield,D.L. (1998) Rabbit β-globin is extended beyond its UGA stop codon by multiple suppressions and translational reading gaps. *Biochemistry*, **37**, 10866–10870.

Craigen,W.J. and Caskey,C.T. (1986) Expression of peptide chain release factor 2 requires high-efficiency frameshift. *Nature*, **322**, 273–275.

Danilevskaya,O.N. and Gragerov,A.I. (1980) Curing of *Escherichia coli* K12 plasmids by coumermycin. *Mol. Gen. Genet.*, **178**, 233–235.

Dirheimer,G., Keith,G., Dumas,P. and Westhof,E. (1995) Primary, secondary and tertiary structures of tRNAs. In Soll,D. and RajBhandary,U.L. (eds), *tRNA: Structure, Biosynthesis and Function*. ASM Press, Washington, DC, pp. 93–126.

Farabaugh,P.J. (1996) Programmed translational frameshifting. *Annu. Rev. Genet.*, **30**, 507–528.

Gallant,J.A. and Lindsley,D. (1998) Ribosomes can slide over and beyond 'hungry' codons, resuming protein chain elongation many nucleotides downstream. *Proc. Natl Acad. Sci. USA*, **95**, 13771–13776.

Gaur,R.K., Hanne,A., Conrad,F., Kahle,D. and Krupp,G. (1996) Differences in the interaction of *Escherichia coli* RNase P RNA with tRNAs containing a short or a long extra arm. *RNA*, **2**, 674–681.

Gay,P., Le Coq,D., Steinmetz,M., Ferrari,E. and Hoch,J.A. (1983) Cloning structural gene *sacB*, which codes for exoenzyme levansucrase of *Bacillus subtilis*: expression of the gene in *Escherichia coli*. *J. Bacteriol.*, **153**, 1424–1431.

Gay,P., Le Coq,D., Steinmetz,M., Berkelman,T. and Kado,C.I. (1985) Positive selection procedure for entrapment of insertion sequence elements in gram-negative bacteria. *J. Bacteriol.*, **164**, 918–921.

Gesteland,R.F. and Atkins,J.F. (1996) Recoding: dynamic reprogramming of translation. *Annu. Rev. Biochem.*, **65**, 741–768.

Green,R. and Noller,H.F. (1997) Ribosomes and translation. *Annu. Rev. Biochem.*, **66**, 679–716.

Grosjean,H., Soll,D.G. and Crothers,D.M. (1976) Studies of the complex between transfer RNAs with complementary anticodons. I. Origins of enhanced affinity between complementary triplets. *J. Mol. Biol.*, **103**, 499–519.

Herbst,K.L., Nichols,L.M., Gesteland,R.F. and Weiss,R.B. (1994) A mutation in ribosomal protein L9 affects ribosomal hopping during translation of gene 60 from bacteriophage T4. *Proc. Natl Acad. Sci. USA*, **91**, 12525–12529.

Hirsh,D. (1971) Tryptophan transfer RNA as the UGA suppressor. *J. Mol. Biol.*, **58**, 439–458.

Huang,W.M., Ao,S.Z., Casjens,S., Orlandi,R., Zeikus,R., Weiss,R., Winge,D. and Fang,M. (1988) A persistent untranslated sequence within bacteriophage T4 DNA topoisomerase gene *60*. *Science*, **239**, 1005–1012.

Kane,J.F., Violand,B.N., Curran,D.F., Staten,N.R., Duffin,K.L. and Bogosian,G. (1992) Novel in-frame two codon translational hop during synthesis of bovine placental lactogen in a recombinant strain of *Escherichia coli*. *Nucleic Acids Res.*, **20**, 6707–6712.

Karim,A.M. and Thompson,R.C. (1986) Guanosine 5′-*O*-(3-thiotriphosphate) as an analog of GTP in protein biosynthesis. The effects of temperature and polycations on the accuracy of initial recognition of aminoacyl-tRNA ternary complexes by ribosomes. *J. Biol. Chem.*, **261**, 3238–3243.

Lawes,M. and Maloy,S. (1995) MudSacI, a transposon with strong selectable and counterselectable markers: use for rapid mapping of chromosomal mutations in *Salmonella typhimurium*. *J. Bacteriol.*, **177**, 1383–1387.

Li,Z. and Deutscher,M.P. (1996) Maturation pathways for *E.coli* tRNA precursors: a random multienzyme process *in vivo*. *Cell*, **86**, 503–512.

Li,Z., Pandit,S. and Deutscher,M.P. (1998) Polyadenylation of stable RNA precursors *in vivo*. *Proc. Natl Acad. Sci. USA*, **95**, 12158–12162.

Maldonado,R. and Herr,A.J. (1998) Efficiency of T4 gene *60* translational bypassing. *J. Bacteriol.*, **180**, 1822–1830.

Manch-Citron,J.N. and London,J. (1994) Expression of the *Prevotella loescheii* adhesin gene (*plaA*) is mediated by a programmed frameshifting hop. *J. Bacteriol.*, **176**, 1944–1948.

Miller,J.H. (1972) *Experiments in Molecular Genetics*. Cold Spring Harbor Laboratory Press, Cold Spring Harbor, NY.

Miller,J.H. (1992) *A Short Course In Bacterial Genetics*. Cold Spring Harbor Laboratory Press, Cold Spring Harbor, NY.

Moras,D., Comarmond,M.B., Fischer,J., Weiss,R., Thierry,J.C., Ebel,J.P. and Giege,R. (1980) Crystal structure of yeast tRNA^{Asp}. *Nature*, **288**, 669–674.

Murgola,E.J. and Pagel,F.T. (1980) Codon recognition by glycine transfer RNAs of *Escherichia coli in vivo*. *J. Mol. Biol.*, **138**, 833–844.

Neidhardt,F.C., Bloch,P.L. and Smith,D.F. (1974) Culture medium for enterobacteria. *J. Bacteriol.*, **119**, 736–747.

O'Connor,M. (1998) tRNA imbalance promotes –1 frameshifting via near-cognate decoding. *J. Mol. Biol.*, **279**, 727–736.

O'Connor,M., Gesteland,R.F. and Atkins,J.F. (1989) tRNA hopping: enhancement by an expanded anticodon. *EMBO J.*, **8**, 4315–4323.

O'Connor,M., Thomas,C.L., Zimmermann,R.A. and Dahlberg,A.E. (1997) Decoding fidelity at the ribosomal A and P sites: influence of mutations in three different regions of the decoding domain in 16S rRNA. *Nucleic Acids Res.*, **25**, 1185–1193.

O'Mahony,D.J., Hughes,D., Thompson,S. and Atkins,J.F. (1989a) Suppression of a –1 frameshift mutation by a recessive tRNA suppressor which causes doublet decoding. *J. Bacteriol.*, **171**, 3824–3830.

O'Mahony,D.J., Mims,B.H., Thompson,S., Murgola,E.J. and Atkins,J.F. (1989b) Glycine tRNA mutants with normal anticodon loop size cause –1 frameshifting. *Proc. Natl Acad. Sci. USA*, **86**, 7979–7983.

Pagel,F.T., Tuohy,T.M., Atkins,J.F. and Murgola,E.J. (1992) Doublet translocation at GGA is mediated directly by mutant tRNA$_2^{Gly}$. *J. Bacteriol.*, **174**, 4179–4182.

Pape,T., Wintermeyer,W. and Rodnina,M.V. (1998) Complete kinetic mechanism of elongation factor Tu-dependent binding of aminoacyl-tRNA to the A site of the *E.coli* ribosome. *EMBO J.*, **17**, 7490–7497.

Pierce,J.C., Sauer,B. and Sternberg,N. (1992) A positive selection vector for cloning high molecular weight DNA by the bacteriophage P1 system: improved cloning efficacy. *Proc. Natl Acad. Sci. USA*, **89**, 2056–2060.

Qian,Q., Li,J.N., Zhao,H., Hagervall,T.G., Farabaugh,P.J. and Bjork,G.R. (1998) A new model for phenotypic suppression of frameshift mutations by mutant tRNAs. *Mol. Cell*, **1**, 471–482.

Ried,J.L. and Collmer,A. (1987) An nptI-sacB-sacR cartridge for constructing directed, unmarked mutations in gram-negative bacteria by marker exchange–eviction mutagenesis. *Gene*, **57**, 239–246.

Riyasaty,S. and Atkins,J.F. (1968) External suppression of a frameshift mutant in *Salmonella*. *J. Mol. Biol.*, **34**, 541–557.

Roberts,J.W. and Carbon,J. (1975) Nucleotide sequence studies of normal and genetically altered glycine transfer ribonucleic acids from *Escherichia coli*. *J. Biol. Chem.*, **250**, 5530–5541.

Rodnina,M.V., Fricke,R. and Wintermeyer,W. (1994) Transient conformational states of aminoacyl-tRNA during ribosome binding catalyzed by elongation factor Tu. *Biochemistry*, **33**, 12267–12275.

Romby,P., Carbon,P., Westhof,E., Ehresmann,C., Ebel,J.P., Ehresmann,B. and Giege,R. (1987) Importance of conserved residues for the conformation of the T-loop in tRNAs. *J. Biomol. Struct. Dyn.*, **5**, 669–687.

Samuelsson,T., Axberg,T., Boren,T. and Lagerkvist U. (1983) Unconventional reading of the glycine codons. *J. Biol. Chem.*, **258**, 13178–13184.

Schultz,D.W. and Yarus,M. (1994) tRNA structure and ribosomal function. I. tRNA nucleotide 27–43 mutations enhance first position wobble. *J. Mol. Biol.*, **235**, 1381–1394.

Simons,R.W., Houman,F. and Kleckner,N. (1987) Improved single and multicopy lac-based cloning vectors for protein and operon fusions. *Gene*, **53**, 85–96.

Singer,M. *et al.* (1989) A collection of strains containing genetically linked alternating antibiotic resistance elements for genetic mapping of *Escherichia coli*. *Microbiol. Rev.*, **53**, 1–24.

Smith,D. and Yarus,M. (1989) Transfer RNA structure and coding specificity. II. A D-arm tertiary interaction that restricts coding range. *J. Mol. Biol.*, **206**, 503–511.

Sprinzl,M., Horn,C., Brown,M., Ioudovitch,A. and Steinberg,S. (1998) Compilation of tRNA sequences and sequences of tRNA genes. *Nucleic Acids Res.*, **26**, 148–153.

Steinmetz,M., Le Coq,D., Aymerich,S., Gonzy-Treboul,G. and Gay,P. (1985) The DNA sequence of the gene for the secreted *Bacillus subtilis* enzyme levansucrase and its genetic control sites. *Mol. Gen. Genet.*, **200**, 220–228.

Svard,S.G. and Kirsebom,L.A. (1993) Determinants of *Escherichia coli* RNase P cleavage site selection: a detailed *in vitro* and *in vivo* analysis. *Nucleic Acids Res.*, **21**, 427–434.

Van Delft,J.H., Schmidt,D.S. and Bosch,L. (1987) The tRNA-tufB operon transcription termination and processing upstream from tufB. *J. Mol. Biol.*, **197**, 647–657.

Varshney,U., Lee,C.P. and RajBhandary,U.L. (1991) Direct analysis of aminoacylation levels of tRNAs *in vivo*. Application to studying recognition of *Escherichia coli* initiator tRNA mutants by glutaminyl-tRNA synthetase. *J. Biol. Chem.*, **266**, 24712–24718.

Wanner,B.L. (1986) Novel regulatory mutants of the phosphate regulon in *Escherichia coli* K-12. *J. Mol. Biol.*, **191**, 39–58.

Watson,J.D., Tooze,J. and Kurtz,D.T. (eds) (1983) *Recombinant DNA: a Short Course*. W.H. Freeman, New York, NY.

Weiss,R.B., Dunn,D.M., Atkins,J.F. and Gesteland,R.F. (1987) Slippery runs, shifty stops, backward steps and forward hops: –2, –1, +1, +2, +5 and +6 ribosomal frameshifting. *Cold Spring Harb. Symp. Quant. Biol.*, **52**, 687–693.

Weiss,R.B., Dunn,D.M., Dahlberg,A.E., Atkins,J.F. and Gesteland,R.F. (1988) Reading frame switch caused by base-pair formation between the 3′ end of 16S rRNA and the mRNA during elongation of protein synthesis in *Escherichia coli*. *EMBO J.*, **7**, 1503–1507.

Weiss,R.B., Huang,W.M. and Dunn,D.M. (1990) A nascent peptide is required for ribosomal bypass of the coding gap in bacteriophage T4 gene *60*. *Cell*, **62**, 117–126.

Westhof,E., Dumas,P. and Moras,D. (1985) Crystallographic refinement of yeast aspartic acid transfer RNA. *J. Mol. Biol.*, **184**, 119–145.
Yarus,M. (1982) Translational efficiency of transfer RNAs: uses of an extended anticodon. *Science*, **218**, 646–652.
Yarus,M. and Smith,D. (1995) tRNA on the ribosome: a waggle theory. In Soll,D. and RajBhandary,U.L. (eds), *tRNA: Stucture, Biosynthesis and Function*. ASM Press, Washington, DC, pp. 443–470.
Yarus,M., Cline,S., Raftery,L., Wier,P. and Bradley,D. (1986a) The translational efficiency of tRNA is a property of the anticodon arm. *J. Biol. Chem.*, **261**, 10496–10505.
Yarus,M., Cline,S.W., Wier,P., Breeden,L. and Thompson,R.C. (1986b) Actions of the anticodon arm in translation on the phenotypes of RNA mutants. *J. Mol. Biol.*, **192**, 235–255.

Received February 15, 1999; revised and accepted March 22, 1999